

- (8) Masuda, T.; Tang, B.-Z.; Higashimura, T.; Yamaoka, H. *Macromolecules* **1985**, *18*, 2369.
- (9) Masuda, T.; Matsumoto, T.; Tang, B.-Z.; Tanaka, A.; Higashimura, T., unpublished data.
- (10) Kang, E. T.; Neoh, K. G.; Masuda, T.; Higashimura, T.; Yamamoto, M. *Polymer* **1989**, *30*, 1328.
- (11) Fujisaka, T.; Suezaki, M.; Koremoto, T.; Inoue, T.; Masuda, T.; Higashimura, T. *Polym. Prepr. Jpn.* **1989**, *38* (3), 797.
- (12) (a) Brandsma, L.; Hommes, H.; Verkruijsse, H. D.; de Jong, R. L. P. *Recl. Trav. Chim. Pays-Bas* **1985**, *104*, 226. (b)

Brandsma, L.; Verkruijsse, H. D. *Synthesis of Acetylenes, Allenes and Cumulenes*; Elsevier: Amsterdam, 1981; p 85.

Registry No. PhC≡CH, 536-74-3; Me₃SiCl, 75-77-4; Me₃SiC₆H₄-o-C≡CSiMe₃, 62618-20-6; Me₃SiC₆H₄-o-C≡CH, 78905-09-6; WCl₆, 13283-01-7; (o-Me₃SiPA) (homopolymer), 112754-88-8; (o-Me₃SiPA) (SRU), 124943-12-0; Ph₄Sn, 595-90-4; MoCl₅, 10241-05-1; W(CO)₆, 14040-11-0; NbCl₅, 10026-12-7; Et₃SiH, 617-86-7; Ph₃SiH, 789-25-3; n-Bu₄Sn, 1461-25-2; Ph₃Sb, 603-36-1; Ph₃Bi, 603-33-8.

Microstructural Evolution of a Silicon Oxide Phase in a Perfluorosulfonic Acid Ionomer by an in Situ Sol-Gel Reaction.

2. Dielectric Relaxation Studies

K. A. Mauritz* and I. D. Stefanithis

*Department of Polymer Science, University of Southern Mississippi,
Southern Station Box 10076, Hattiesburg, Mississippi 39406-0076. Received May 16, 1989;
Revised Manuscript Received August 29, 1989*

ABSTRACT: Microcomposite membranes were produced via the in situ diffusion-controlled and acid-catalyzed sol-gel reaction for tetraethoxysilane in prehydrated and methanol-swollen Nafion perfluorosulfonic acid films. The storage and loss components of the complex dielectric constants of these modified membranes were determined over the frequency range 5 Hz to 13 MHz as a function of invasive silicon oxide content and temperature. The large storage components displayed by these microcomposites suggest the action of an interfacial polarization which, in turn, suggests the persistence of a microphase-separated, i.e. clustered, morphology after incorporation of the silicon oxide structures. Long-range motions of charge, tentatively attributed to the intercluster hopping of protons, is strongly manifest on the loss spectra. A parameter, n , which is extracted from the isothermal loss component vs frequency spectra, is reflective of the degree of connectivity of underlying charge pathway networks. n vs temperature or silicon oxide content relationships are then viewed as coarsely indicative of the evolution of the microcomposite morphological texture with the variance of these two factors. The observed range of n is broad, which suggests considerable morphological differentiation, and definite trends in this parameter are seen. While n vs filler level at constant temperature exhibits organized but complex behavior, n vs temperature at constant filler level plots appear as distinctly increasing curves except at the highest loading. A structural-mechanistic assignment of three absorption peaks detected beyond the dc conduction region for the microcomposites as well as for the unfilled acid precursors is not evident at this time, although the lowest frequency peak might be due to the relaxation of polarization across clusters.

Introduction

Mauritz et al. have recently reported on the formulation of unique microcomposite membranes via the in situ growth of a dispersed silicon oxide phase in Nafion¹ perfluorosulfonic acid films.^{2,3} In short, an acid-catalyzed, diffusion-controlled, sol-gel reaction for tetraethoxysilane (TEOS) was affected in prehydrated and alcohol-swollen membranes that were immersed in TEOS/alcohol solutions for various times after which the membranes were dried and annealed in controlled fashion to optimize the cross-linking of the in situ gel network. It was initially hypothesized and is now becoming increasingly clear that the final morphology of the invasive inorganic phase is ordered by the original polar/nonpolar phase-separated morphology presented by the perfluorosulfonic acid matrix.

Our previous FT-IR, ²⁹Si NMR, and mechanical tensile studies portray an internal silicon oxide network structure that is rather heterogeneous on a molecular scale, being increasingly less interconnected but more strained with increasing gel content. While it appears that silicon oxide clusters initially grow in single isolation, it was

suggested that a percolation threshold is eventually reached at which the clusters become interknitted by (≡SiO)_n chains over macroscopic dimensions.

In this work, we report results of the characterization of these hybrid materials by means of dielectric relaxation spectroscopy. We had previously investigated the nature of short- and long-range ion motions and their relationship to the ion-clustered morphology in identical Nafion perfluorosulfonate membranes imbibed with a variety of aqueous electrolytes over ranges of concentration and temperature.⁴⁻⁷ The mechanistic concepts that have emerged from our investigations of these systems have provided valuable insight for the interpretation of the similar dielectric relaxation spectra reported for the closely related silicon oxide-filled Nafion systems in this work.

In general terms, compositional segregation or phase separation with controlled interfacial geometry presents an opportunity to design materials with interesting dielectric or charge transport properties that are not possible with microstructurally homogeneous materials. Owing to considerable differences in electrical polarizabilities

and charge mobilities across the boundaries between distinct phases, an accumulation followed by dissipation of net charge at these interfaces along the direction of an applied electric field during each half-cycle of field oscillation will occur. This cooperative relaxation of interfacial polarization will be most intense and give rise to a dielectric absorption peak at a characteristic frequency, at a given fixed temperature. An electric field-induced large-scale charge separation can generate a very high dipole moment per unit volume in these systems that will give rise to an enormous macroscopic dielectric constant either in a static field or at low frequencies in oscillating fields. It has been established by both theory⁸ and experiment⁹ that the dielectric constant for heterogeneous systems is greater than that for each phase taken separately.

While the above discussion is concerned with the rather *short-ranged* motions of ions that are implicated in the fluctuation of the polarization of ca. 40 Å in diameter hydrated ionic clusters in Nafion membranes at high frequencies, *long-range*, i.e. intercluster, ion motions become increasingly manifest with decreasing applied frequency. In particular, the dielectric loss (ϵ'') spectra in the low-frequency (f) region of Nafion sulfonate membranes incorporating aqueous electrolytes has been seen to vary as f^{-n} where $0 < n < 1$.⁴⁻⁶ n is a distinct function of ionic species and concentration as well as system temperature.⁷

Mauritz⁷ has recently attempted to relate the power n to (a) theories of processes that are fractal in space and time,¹⁰ (b) the theory of the dispersive transport of charge carriers in disordered materials,¹¹ and (c) the cluster theory of the anomalous low-frequency dielectric dispersion phenomenon.^{12,13} It was suggested that while these related theories in themselves presently do not possess a sufficient level of microstructural detail that would permit discrimination between different materials, experimentally extracted values of n might nonetheless be used as rough qualitative indices of morphological regularity or "texture" over an array of ionic clusters or as a measure of the degree of connectivity of the overall charge pathway network.

In general interpretation, $n = 1$ corresponds to an "ideal" situation wherein charge conducting pathways span the entire sample dimensions in continuous fashion and charge drift is dominant over random hopping for low applied electric fields. $n < 1$ indicates systems having random charge conducting paths that may or may not intersect each other. The degree of topological imperfection increases as n decreases as dead ends or charge traps become more numerous on the conductivity grid. $n = 1/2$ is suggestive of diffusion control and tortuous charge pathways. We will employ these general concepts in our analysis of the dielectric relaxation spectra of silicon oxide filled Nafion perfluorosulfonate membranes.

While it will be rather evident in the presented spectra that long-range charge conduction must take place in these microcomposite membranes, a short comment on the nature of the underlying charge carriers is now in order. In our earlier dielectric relaxation experiments with electrolyte-imbibed Nafion films, it was quite obvious that mobile hydrated cations and anions were the main contributors to the observed dc conduction.⁴⁻⁶ While the identification of a corresponding long-range charge conduction mechanism within the more ubiquitous silicon oxide in Nafion system is clearly not as straightforward, the following tentative proposal is offered. Our previous infrared and ²⁹Si solid-state NMR structural stud-

ies of the microcomposite membranes strongly indicate that the invasive silicon oxide network is rather unconnected, is open, and contains a high relative population of unreacted OH groups.^{2,3} If we then reasonably assume that these abundant residual OH groups can act as strong hydration sites, as is the case for conventional silica gel powders which have high specific surface areas, *protons* might be envisioned as hopping along the hydrogen bonds of water molecules, many of which are bound in this way. Of course, the sorbed water is "incidental" and is incorporated to an unknown and somewhat uncontrolled degree, although all samples have in fact been exposed to the same atmospheric humidity for approximately the same short times in rapid transference from dry storage to the dielectric test cell. Also, within the realm of this proposed scheme, it would be reasonable to expect that the (proton) charge carrier density is considerably lower than that which exists in the aqueous electrolyte-imbibed membranes and that the long-range charge carrier hopping mobility might be lower, as well. Mainly for these reasons, comparatively lower values of the parameter n might be anticipated.

Experimental Section

Although the formulation of microcomposite membranes via the in situ sol-gel reaction of TEOS in prehydrated and alcohol-swollen Nafion sulfonic acid films has been presented in an earlier report,² the procedural details will be repeated here in the interest of completeness and to avoid interpretive ambiguity. The membranes used in this work were of 1100 equivalent weight and 7 mil nominal thickness ("Nafion 117").

While all the membranes were received as being nominally in the acid form, we nonetheless sought to ensure complete protonation of the sulfonate groups by soaking in 1.0 M HCl for 24 h at room temperature. Then, all the membranes were removed, surface-blotted, and soaked in stirred deionized water for 24 h at 40 °C in order to leach out excess HCl and affect the mole ratio of $H^+ : SO_3^- = 1:1$. Therefore, the remaining intended catalytic protons are membrane-bound and reasonably confined to the ca. 40 Å in size polar clusters. The deionized water bath was refreshed every 8 h over this time period to promote complete free acid extraction. Then, the films were removed, blotted, and air-dried in the atmosphere for 5 h, dried under vacuum for 24 h, and finally heated at 120 °C also under vacuum.

Owing to the common fact that Nafion materials exhibit swelling hysteresis as well as the fact that membrane physical properties are rather sensitive to ionic form and water content, we reduced all samples to this *standard initial state* prior to affecting the in situ sol-gel reaction to hopefully maximize resultant structure/property reproducibility.

All initialized membranes were preswollen (i.e. equilibrated) in stirred 2:1 (vol/vol) methanol/water solutions for 5 h at 22 °C. This presorbed water initiates the in situ sol-gel reaction given the subsequent uptake of TEOS which is introduced in quantities such that $H_2O/TEOS = 4:1$ (mol/mol). In addition to having just enough water initially available for complete alkoxide hydrolysis, more water is of course generated during the ensuing polyfunctional condensation. Solutions of 1.5:1 (vol/vol) TEOS/methanol were then added to the flasks that already contained the acid-form membranes in equilibrium with the above methanol/water solutions and these flasks were always stoppered after liquids were added.

The membranes were then removed from these complex multicomponent reactive solutions after they were exposed to TEOS for 1, 5, 10, 15, and 20 min. While the sol-gel reaction continues within the membranes after these times of removal, the diffusion-controlled exchange of reactants and solvent across the membrane/solution interface ceases. Therefore, the time between the addition of TEOS and the removal of the membrane from solution will be referred to as "diffusion time" rather than as reaction time. Upon removal from the solutions, the films were surface-blotted dry and finally placed under vacuum for 24 h,

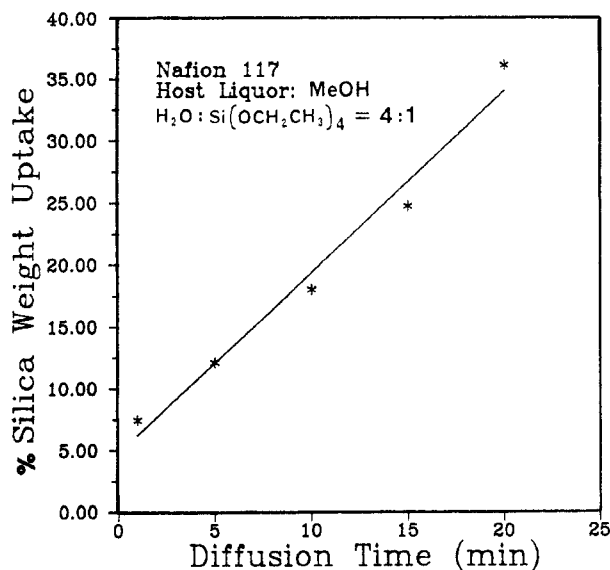


Figure 1. Percent silicon oxide weight uptake of Nafion 1100 equivalent weight sulfonic acid membranes, after drying-annealing, vs time of diffusion of TEOS from methanol solution.

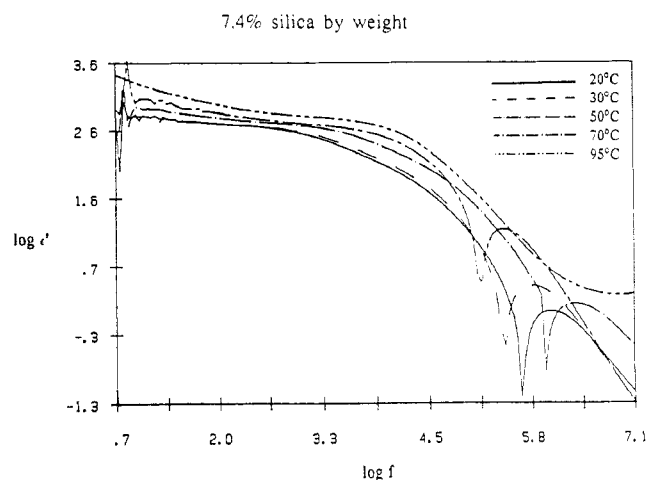


Figure 2. ϵ' vs f for microcomposite membranes incorporating 7.44% silicon oxide at the indicated constant temperatures.

the last 2 h of which were spent in heating at 110 °C to remove trapped volatiles as well as to promote further silicon oxide network condensation.

Save for the initialization protocol, the entire procedure up to the last heating step was carried out at 22 °C.

The percent weight uptakes, relative to the initial dry acid-form, for the final dried-annealed samples are seen plotted against diffusion time in Figure 1. We note that the graph is reasonably linear, as also reported for earlier similar microcomposite preparations.^{2,3}

These samples were then all stored in a desiccator prior to the electrical impedance measurements.

The experimental configuration used to determine the dielectric relaxation spectra of the microcomposite membranes in the frequency range 5 Hz to 13 MHz at fixed temperatures is built around a Hewlett-Packard 4192A impedance analyzer, which has been adequately described in a previous communication.⁴ Dielectric relaxation spectra (ϵ' and ϵ'' vs f) were obtained for each of the above six samples at the constant temperatures 20, 30, 50, 70 and 95 °C.

Results and Discussion

Displayed in Figures 2 and 3 are the dielectric storage and loss spectra, respectively, at the indicated temperatures for microcomposite membranes containing 7.44% silicon oxide. In Figure 2 it is seen that the ϵ_0 , i.e. low-

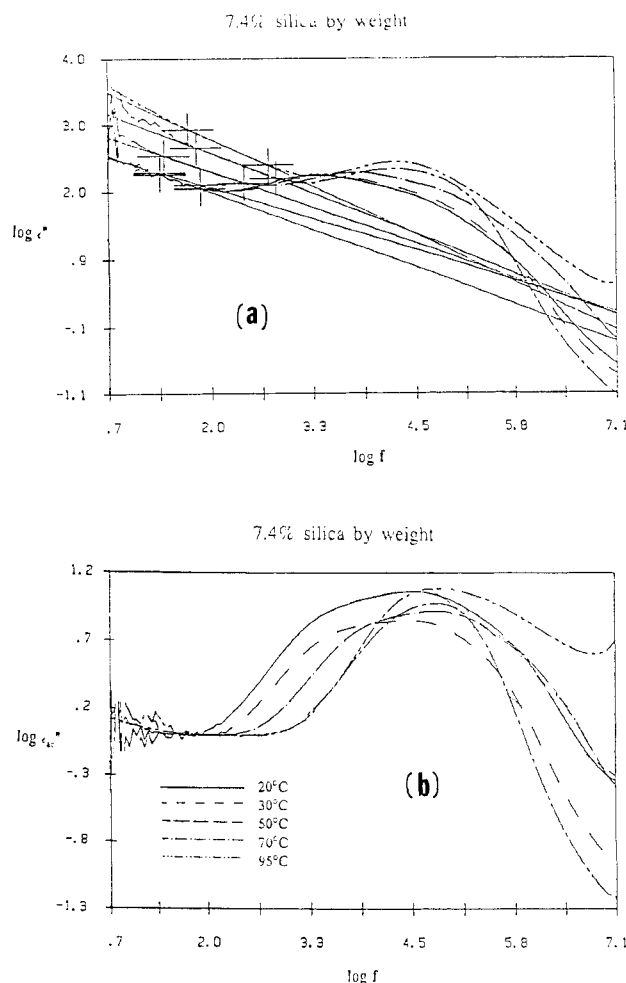


Figure 3. (a) ϵ'' vs f for microcomposite membranes incorporating 7.44% silicon oxide at the indicated constant temperatures. Also shown are the best-fit lines (ϵ''_{dc}) in the dc conduction region. (b) Same as (a) but for $\epsilon''_{ac} = \epsilon'' - \epsilon''_{dc}$.

frequency-limiting values of ϵ' , are rather high at all temperatures. Also, there appears to be a sharp dip in ϵ' , followed by its recovery, at higher frequencies at all temperatures but 95 °C. There are two distinctive general features on all the loss spectra shown in Figure 3. First, there is a low-frequency region over which $\log \epsilon'' \propto \log f$ which becomes better defined and broader with increasing temperature. This region is clearly dominated by dc conduction and the linear slope is the earlier discussed parameter n which is thought to be reflective of the degree of intercluster charge hopping connectivity.

Second, to the right of the linear segment is an absorption peak that becomes progressively narrower and shifts slightly to higher frequencies with increasing temperature. The absorption peaks for these as well as for the remaining samples are seen more distinctly after the dc component is subtracted from ϵ'' at each f . Having performed this operation, the pure relaxation peaks are as shown in Figure 3b.

In Figures 4 and 5 are the storage and loss spectra, respectively, at the same temperatures as above, for membranes incorporating 12.1% silicon oxide. Again, the values of ϵ_0 are high, being approximately equal to the values seen for the previous 7.44% samples at the same temperatures, and clearly increase with increasing temperature. Again, on the ϵ'' vs f curves, there exists at each temperature a linear dc conduction region and a major peak. This major peak, however, differs greatly from those seen in Figure 3 in appearing at considerably higher frequen-

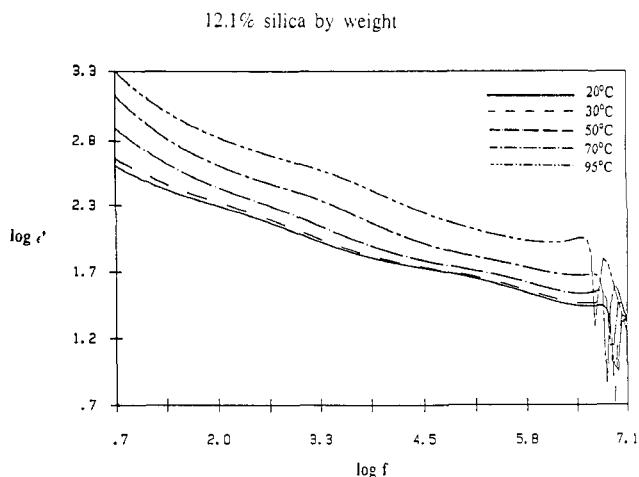


Figure 4. ϵ' vs f for microcomposite membranes incorporating 12.1% silicon oxide at the indicated constant temperatures.

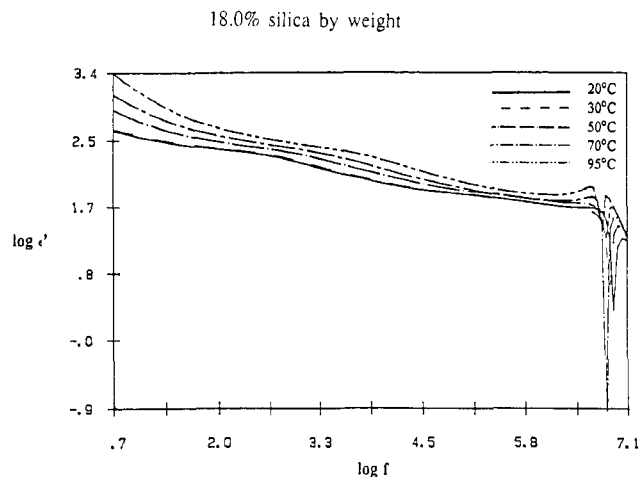


Figure 6. ϵ' vs f for microcomposite membranes incorporating 18.0% silicon oxide at the indicated constant temperatures.

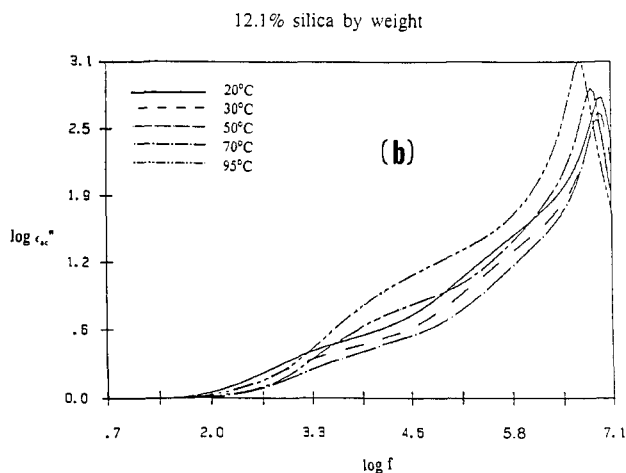
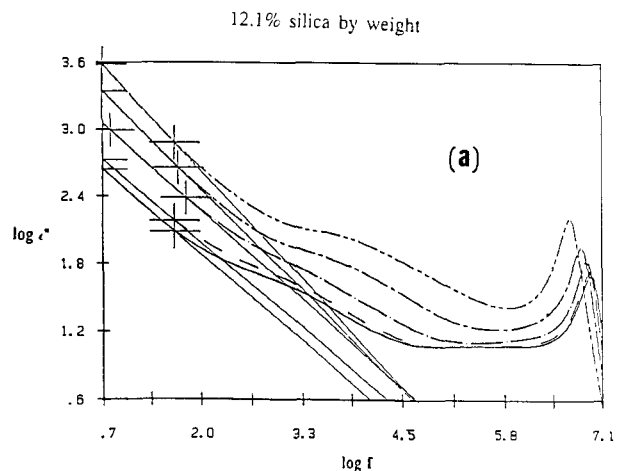


Figure 5. (a) ϵ'' vs f for microcomposite membranes incorporating 12.1% silicon oxide at the indicated constant temperatures. Also shown are the best-fit lines (ϵ''_{dc}) in the dc conduction region. (b) Same as (a) but for $\epsilon''_{ac} = \epsilon'' - \epsilon''_{dc}$.

cies, with a slight progressive shift to lower rather than higher frequencies with increasing temperature, and in being much more narrow. It also appears that a broad and less intense peak is steadily evolving between these two features with increasing temperature. This secondary, rather flat, peak, in fact, is situated in the region of the major broad peak in Figure 3, although it is less intense. Moreover, the final upswing in ϵ'' at the highest tested frequencies that is observed at 95 °C in Figure 3 suggests that there is a second peak, albeit off-scale, for the

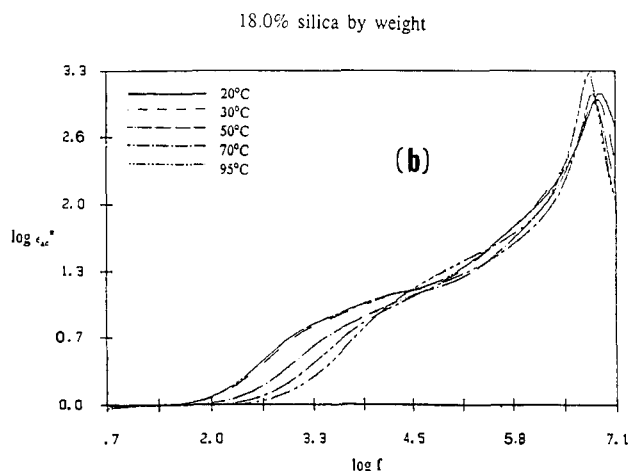
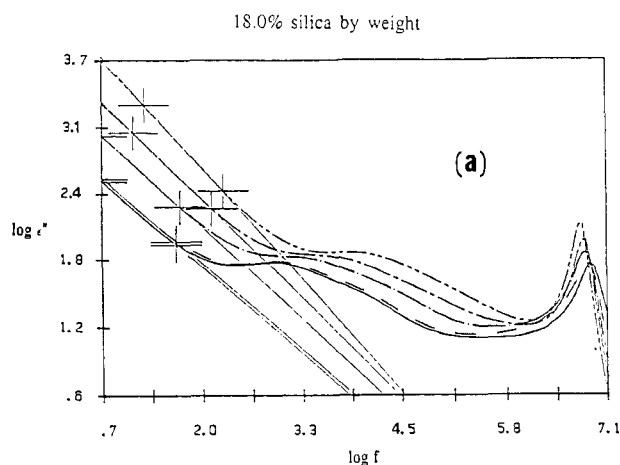


Figure 7. (a) ϵ'' vs f for microcomposite membranes incorporating 18.0% silicon oxide at the indicated constant temperatures. Also shown are the best-fit lines (ϵ''_{dc}) in the dc conduction region. (b) Same as (a) but for $\epsilon''_{ac} = \epsilon'' - \epsilon''_{dc}$.

7.44% samples as well. In other words, it would appear that for these two silicon oxide contents there are at least two dielectric relaxations that are operative.

An inspection of the isothermal spectra for membranes containing 18.0% silicon oxide, displayed in Figures 6 and 7, leads to the same general description offered above for the 12.1% samples save for the fact that the broad peak at intermediate frequencies is now relatively more prominent. The enhancement of ϵ_0 and slight shift

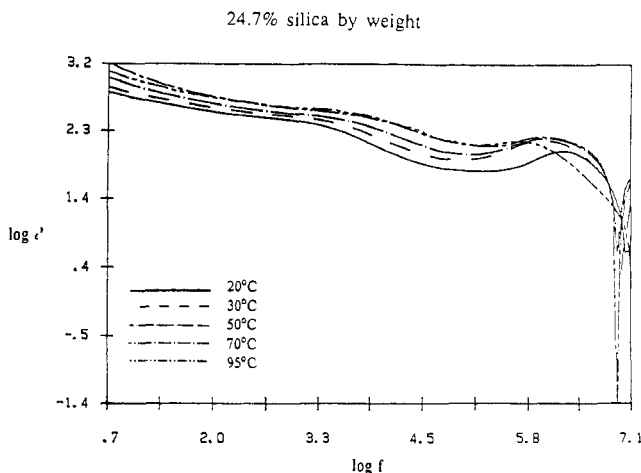


Figure 8. ϵ' vs f for microcomposite membranes incorporating 24.7% silicon oxide at the indicated constant temperatures.

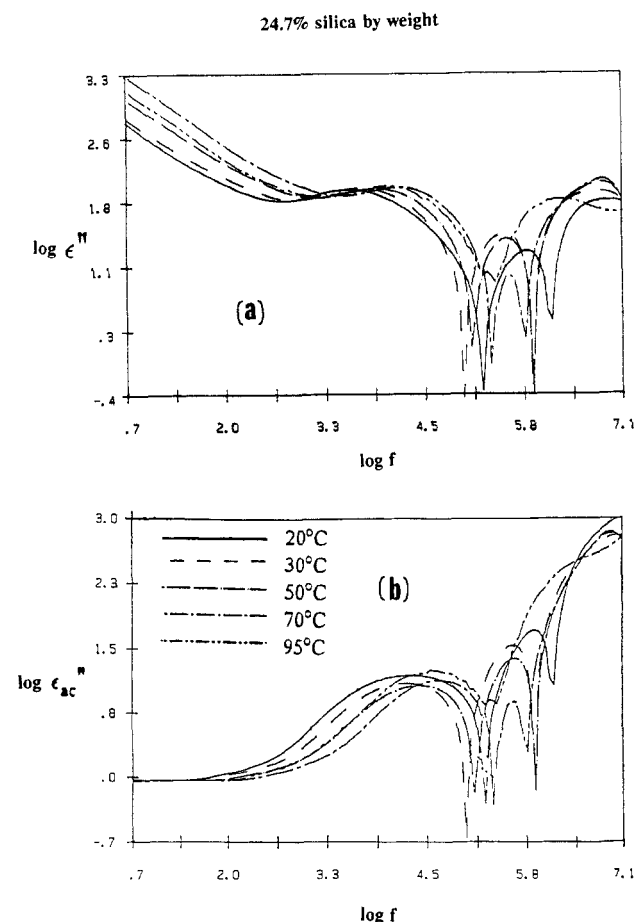


Figure 9. (a) ϵ'' vs f for microcomposite membranes incorporating 24.7% silicon oxide at the indicated constant temperatures. The best-fit lines (ϵ''_{dc}) in the dc conduction region have been omitted in this case to permit visual discrimination between the curves. (b) Same as (a) but for $\epsilon''_{ac} = \epsilon'' - \epsilon''_{dc}$.

of a narrow high-frequency peak to lower frequencies, with increasing temperature, are seen again. The broad peak, on the other hand, is steadily shifted to higher frequencies with advancing temperature.

At the 24.7% inorganic filler level, the spectra, seen in Figures 8 and 9, have become more complex with the existence of three relaxation peaks beyond the dc conduction region. There appears, between the high- and low-frequency peaks, a third peak that gradually disappears with increasing temperature. On inspection of Figure 9, it is not clear as to whether this third intermedi-

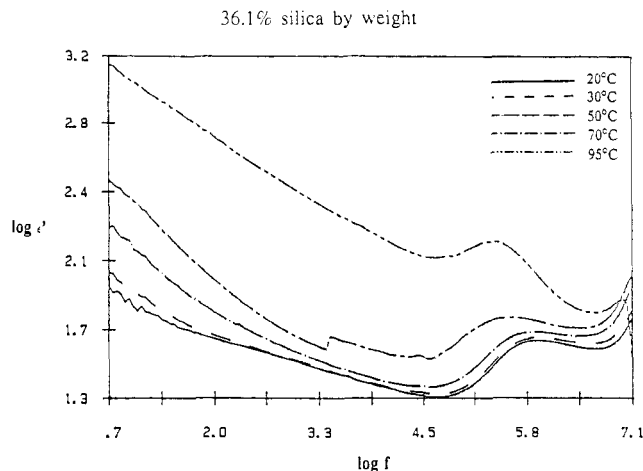


Figure 10. ϵ' vs f for microcomposite membranes incorporating 36.1% silicon oxide at the indicated constant temperatures.

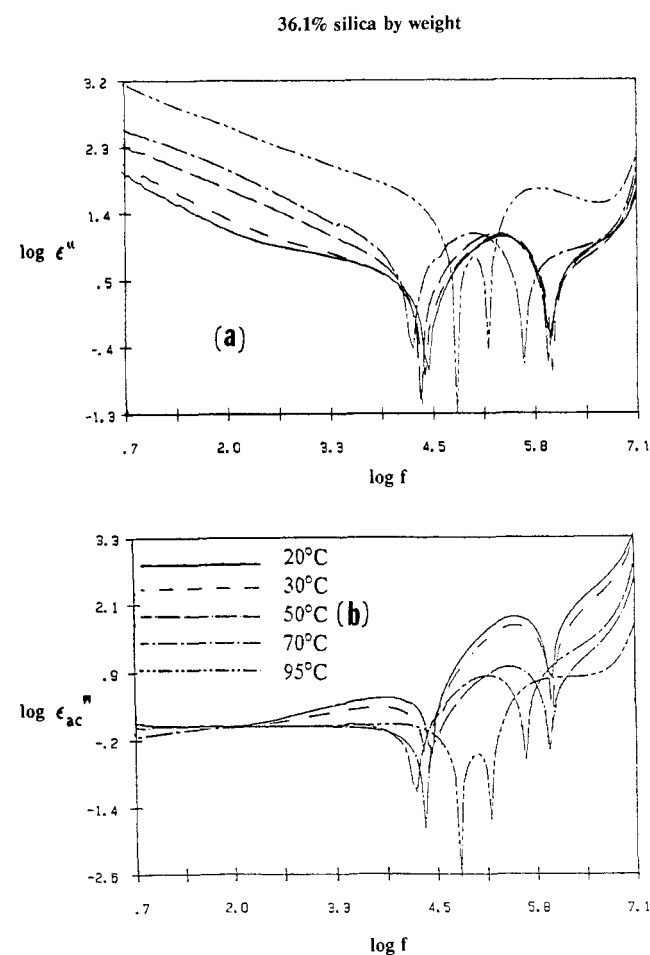


Figure 11. (a) ϵ'' vs f for microcomposite membranes incorporating 36.1% silicon oxide at the indicated constant temperatures. The best-fit lines (ϵ''_{dc}) in the dc conduction region have been omitted in this case to permit visual discrimination between the curves. (b) Same as (a) but for $\epsilon''_{ac} = \epsilon'' - \epsilon''_{dc}$.

ate relaxation is actually being mechanistically suppressed or is merely being engulfed by the high-frequency peak which is progressively broadened toward lower frequencies. The low-frequency peak suffers a shift to higher frequencies with increased temperature, as before.

At the highest weight uptake, 36.1%, the following observations of the storage and loss spectra in Figures 10 and 11 are made. Again, ϵ_0 gradually increases with increasing temperature to a value that is comparable to the rea-

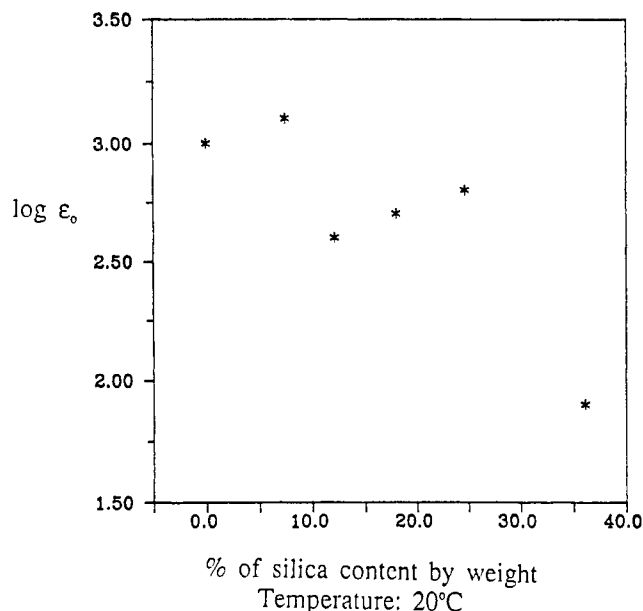


Figure 12. Low-frequency-limiting dielectric constant, ϵ_0 , vs percent silicon oxide for microcomposites at 20 °C.

sonably identical 95 °C values observed for all the lesser filled membranes. ϵ_0 , however, starts from a significantly lower value at 20 °C for the 36.1% samples than do the values at 20 °C for the samples having lower filler contents, as displayed in Figure 12. In essence, the graph in Figure 12 reflects a rather discontinuous drop in the overall membrane electrical polarizability which, in turn, most likely results from a transition within the microphase-separated morphology. More specifically, one might perhaps think of a silicon oxide/perfluoroorganic interfacial polarization mechanism as being diminished in intensity as the inorganic phase becomes more continuous, that is, as previously isolated silicon oxide microclusters become interknitted by condensation polymerization.

As in the 24.7% filled membranes, the loss spectra, seen in Figure 11, are rather complex and display at least three relaxation peaks beyond the dc conduction-dominated regime. In this case, the aforementioned lowest frequency peak seems to gradually disappear while the dc segment becomes extended with increasing temperature. Perhaps the loss of this relaxation might also be implicated with the disappearance of isolated silicon oxide microclusters, as discussed in the Conclusions. The intermediate frequency loss peak is rather strong at low temperatures but is also diminished at the highest temperature, as was the case for the 24.7% microcomposite.

At the highest frequencies, there appears to be a strong peak, a good part of which is off-scale, on which is a shoulder that becomes more distinctive with increasing temperature.

Let us now examine the behavior of n vs temperature and silicon oxide content. The response of n to temperature for fixed percent weight uptakes is shown in Figure 13. Also graphed for comparison is the curve for a pure "dry" sulfonic acid membrane (0%). Considering experimental error, the fact that n is a derived second-order graphical parameter, and occasional curve intersection, a number of significant conclusions and trends can nonetheless be discerned on inspection of Figure 13.

First, excepting the 36.1% case, there is a general increase in n with increasing temperature. Second, there is an overall rise, followed by a drop in the curves with increasing silicon oxide concentration, the lowest curve corresponding to the lowest concentration. The range

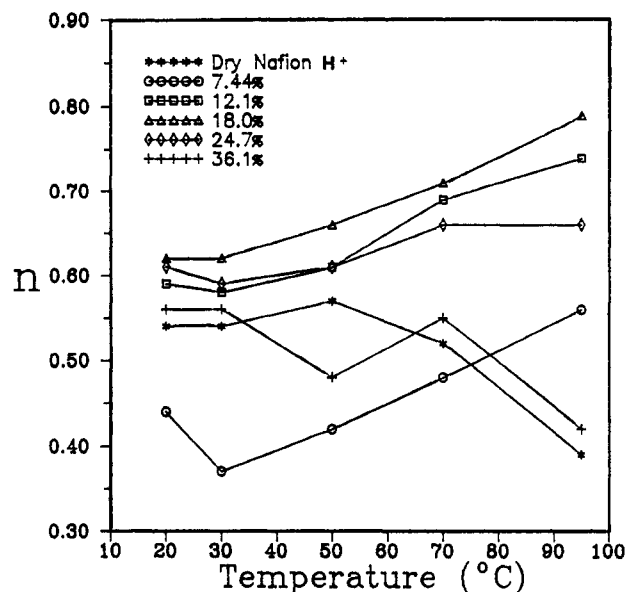


Figure 13. n vs temperature for "dry" Nafion sulfonic acid membranes and for microcomposite membranes having indicated fixed silicon oxide filler levels.

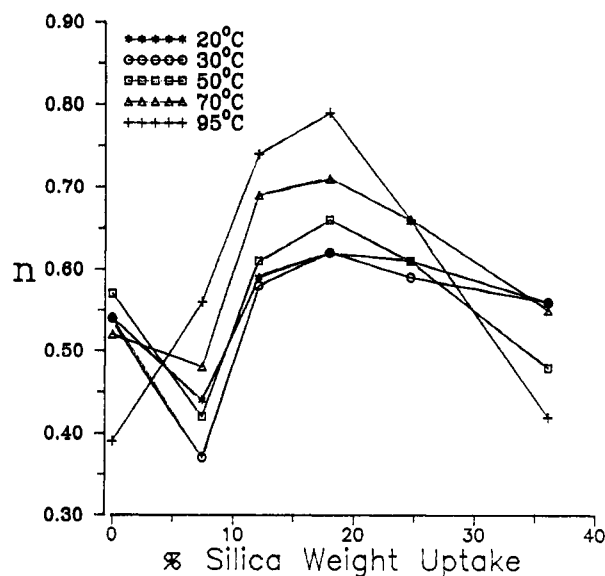


Figure 14. n vs percent silicon oxide for microcomposite membranes at the indicated temperatures.

of n values is broad, indicative of considerable morphological variance. The curve for the pure sulfonic acid membrane has an overall downward trend which, interestingly, closely follows the curve for the membrane having the highest rather than lowest loading, save for the point separation at 50 °C.

Figure 14 is a plot of n vs percent loading at constant temperatures. To be sure, the dependence of n on silicon oxide content is more complicated than its dependence on temperature. Despite this complexity, however, the general pattern of decline followed by rise followed by decline is common to all fixed temperatures.

Before the trends of these spectral features for the filled membranes can be interpreted in terms of an evolving silicon oxide microstructure and molecular mechanisms therein, base-line spectra for the unfilled dry sulfonic acid precursors should be established. Spectra for such control samples in the temperature range 20–95 °C are shown in Figures 15 and 16.

In short, while differing in details, the dielectric responses for filled and unfilled membranes at corresponding tem-

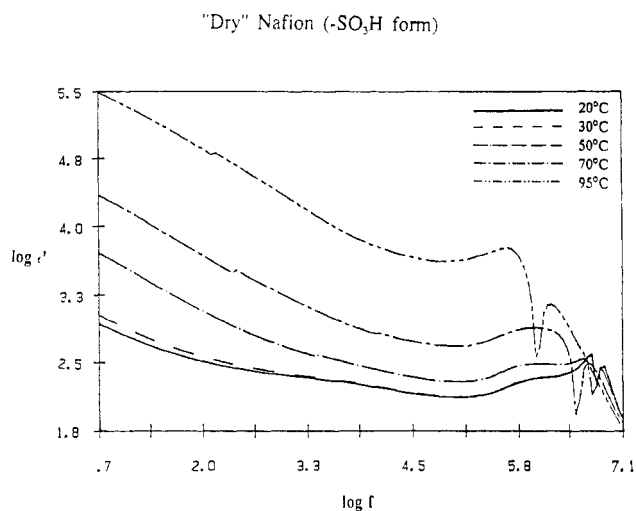


Figure 15. ϵ' vs f for dry, unfilled, Nafion sulfonic acid membranes at the constant indicated temperatures.

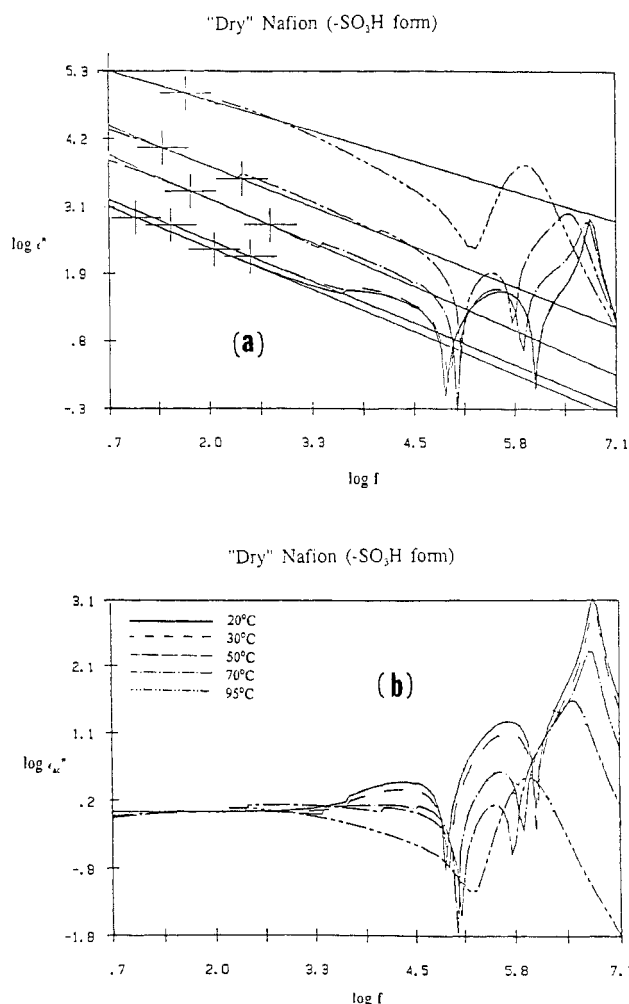


Figure 16. (a) ϵ'' vs f for dry, unfilled, Nafion sulfonic acid membranes at the constant indicated temperatures. Also shown are the best-fit lines (ϵ''_{dc}) in the dc conduction region. (b) Same as (a) but for $\epsilon''_{ac} = \epsilon'' - \epsilon''_{dc}$.

peratures are rather qualitatively similar. ϵ_0 at 20 °C for the pure H^+ form is approximately the same ($\sim 10^3$) as its value for the least filled (7.44% uptake) membrane at 20 °C, as might seem reasonable. On the other hand, ϵ_0 for the H^+ form increases by about 2 orders-of-magnitude on increasing the temperature to 95 °C, whereas the corresponding increase for the 7.44% sample remains within an order of magnitude. The high-temperature limit

of around $10^{5.5}$ for the H^+ form is not attained with any of the filled membranes. Apparently, the H^+ form is more electrically polarizable, i.e. can have induced within it a higher dipole moment per unit volume than that which is possible within any of the filled membranes.

One sees again, in the $\log \epsilon''$ vs $\log f$ plots in Figure 16, a well-defined linear dc conduction-dominated region at lower frequencies. Perhaps it is appropriate to repeat here our earlier observation of the very close behavior of n vs T for the pure H^+ form and that of the highest filled (36.1%) membrane in Figure 13. These results, as well as those discussed in the previous paragraph, will be rationalized in terms of proposed charge carrier mechanisms in the conclusions section.

Surprisingly, there are for the precursor H^+ forms as many loss peaks beyond the dc region as exist on the spectra of the more structurally complex silicon oxide filled membranes. Of the three distinctive relaxations seen in Figure 16, the one appearing at the lowest frequency seems to have effectively disappeared at the temperature of 50 °C and beyond. The intermediate-frequency peak appears to be more persistent but is also extinguished at 95 °C. The most prominent loss peak appears at the highest tested frequencies and is seen to shift to lower frequencies with increasing temperature. Additionally, a shoulder on the low-frequency side of this peak is evident at all but the highest of these temperatures. This high-frequency peak and its progressive shift to lower frequencies with increasing temperature has its counterpart in the spectra of the filled membranes, save for the samples having the highest loading.

Despite these similarities, it is of significant note that the precursor H^+ membrane spectra become progressively simpler while the filled membrane spectra become increasingly more complex with increasing temperature.

Interpretation and Conclusions

A rationalization of the above results, largely in terms of charge-hopping mechanisms operative within a polar/nonpolar microphase-separated morphology, will be presented. To be sure, the qualitative concepts that will now be discussed, which are based upon the limited knowledge of these as well as similar systems, must be considered as tentative.

To begin with, unfilled Nafion sulfonic acid membranes, even in the unhydrated state, are thought to possess a phase-separated morphology consisting of approximately nanometers in size polar clusters within a continuous perfluorocarbon phase.¹⁴ Then, it could be argued, as in the fashion presented in earlier reports of the dielectric responses of various aqueous electrolyte-containing Nafion sulfonate membranes,⁴⁻⁷ that an interfacial electrical polarization can give rise to the very large observed values of ϵ_0 observed in this work. Owing to the presence of the very strong acid functionality and the well-recognized fact that it is very difficult to totally dehydrate Nafion in its very hydrophilic H^+ form, it is quite reasonable to assume that these resins will contain a large population of charge carriers in the form of *mobile protons*. The "incidental" water of hydration will serve to promote the hopping of protons along hydrogen-bonded structures. Of course, the proton mobility would be greater in the sulfonate-rich cluster environment than in the partially crystalline¹⁵ hydrophobic phase. Consequently, an excess of protonic charge at the end of a cluster pointing toward the electric field direction and corresponding protonic charge deficiency at the opposite end will be induced. This polarization, induced over the entire cluster domain, builds up in response to the applied field increase dur-

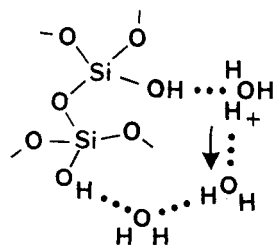


Figure 17. Hypothetical depiction of hydration about OH groups on membrane-incorporated silicon oxide networks and the hopping of protons within clusters of hydrogen-bonded water molecules.

ing the first quarter of a sinusoidal excitation and then dissipates during the following quarter with the process repeating, but in the opposite direction during the remaining two quarter cycles. The degree to which polarization is induced across these clusters, of course, increases with decreasing frequency because the charges will have increasingly longer time intervals during which they can electrodiffusively migrate in the same direction to accumulate at the interface during a quarter cycle of field buildup.

On the other hand, as the frequency of the applied field decreases, an increasingly greater number of *intercluster* proton hopping events will also have time to occur. In other words, long-range charge conductive pathways of progressively greater length are sampled. We believe that this mechanism is responsible for the linear segments of the plots in Figure 16 and that the downturn in their slopes (i.e. n) with increasing temperature, as seen in Figure 13, is reflective of a gradual disruption of the connectivity of proton-conductive pathways. Even the highest values of n for the H^+ precursors, approximately 0.55, are more suggestive of strong diffusion control and tortuous pathways than of charge drift in long-range transport.⁷ We note that a steady downward trend in n with increasing temperature also exists for identical membranes containing very concentrated aqueous NaOH, but the values of n are considerably greater in the latter situation.⁷ Of course, the aqueous NaOH-containing systems contain an abundance of charge carriers by way of hydrated excess Na^+ counterions and associated highly mobile OH^- coions, in addition to SO_3^- -associated Na^+ ions, while the "dry" H^+ forms do not. Perhaps, in a general sense, one might imagine that while increased H^+ mobility is affected on a local level (i.e. *intracluster*, in the vicinity of SO_3^- aggregations) with increased temperature, a greater degree of long-range structural disorder might also be imparted throughout the polymer matrix within which H^+ species are forced to migrate, thus forcing n down toward the value of which is associated with random charge pathways.

We are presently unable to sufficiently rationalize the overall rise followed by the lowering of the n vs T curves with increasing silicon oxide content, as seen in Figure 13. Our earlier discussed spectroscopic characterizations of the silicon oxide phase, suggesting that the incorporated gel is rather unconnected, containing a large relative population of residual OH groups, and in fact becomes gradually less cross-linked with increasing gel content, provide the sole molecular structural information on which an interpretation of the above results can presently be based. Logically assuming then that the abundant OH groups on these rather open silicon oxide networks are hydrated, as depicted in Figure 17, the protons can be visualized to move rather easily within clusters of hydrogen-bonded water molecules and perhaps to hop with greater

difficulty between such noncontiguous water clusters. The initial overall rise of the n vs T curves with increasing silicon oxide content seen for the first three filler levels in Figure 13 might then be explained in terms of the above picture wherein the continuous hydrogen-bonded pathways along which protons can migrate become more extensive. On the other hand, a rationale for the consecutive drops of the n vs T curves for the last two filler levels is not obvious to us. Perhaps by the time a filler level of 24.7% is attained a profound morphological change, such as the onset of the long-range intergrowth of silicon oxide clusters has taken place, as suggested in our earlier studies of this system.²

The following limited SAXS studies of the same microcomposite membranes produced in our laboratory, by Huang et al.,¹⁶ might be relevant in this physical interpretation. In these preliminary studies, a small angle ionic cluster-assigned peak was seen for both filled and unfilled membranes, suggesting that the three-dimensional template action of the original phase-separated Nafion morphology remains intact or undisturbed by the invasion of TEOS and the subsequent hydrolysis-polyfunctional condensation and in situ gel formation that was further promoted by drying-annealing. This scattering peak was seen to diminish with increasing filler content, perhaps as the result of the silicon oxide clusters beginning to grow together. The earlier discussed downturn in the ϵ_0 vs filler level curve at 20 °C (Figure 12) that occurs at the highest loading might be considered, in the light of these SAXS results as well as our mechanical tensile studies, to arise from the loss of a considerable amount of perfluoroorganic/silicon oxide interface through such cluster coalescence. This occurrence would necessarily suppress the interfacial polarization mechanism, thus driving ϵ_0 down.

The overall rise in n with increase in temperature at all filler levels but the highest might simply be due to an enhanced proton mobility that results from thermally activated water molecule reorientations that occur with greater frequency, thereby increasing the rate of water-to-water proton transfers.

The enhancement of ϵ_0 , i.e. membrane polarizability, with increased temperature can be understood for both the unfilled precursor membranes as well as for microcomposites having a given filler level within the general concept of a thermally activated *intracluster* charge carrier mobility. The generally increasing breadth of the linear (dc-dominated) segment in the loss spectra, with increasing temperature, for both filled and unfilled systems would seem to reflect a situation wherein mobile charge carriers are capable of executing progressively greater net *intercluster* displacements in the applied electric field direction at a given frequency owing to a thermally activated intercluster charge-hopping mobility.

The considerable similarity in the loss spectra for unfilled and filled membranes including a seemingly identical multiplicity of peaks as well as the qualitatively similar temperature shifting of corresponding peaks makes it difficult to assign specific spectral features for the filled membranes to aspects of the evolving silicon oxide microstructure. The overall morphological aspect that appears to be common to both precursor and microcomposite forms (save for the highest-filled membranes) is that of phase separation.

For the filled membranes, the gradual shift of the lowest frequency absorption peak to higher frequencies with increasing temperature is somewhat reminiscent of the behavior of the single relaxation peak identified in our

earlier spectra of aqueous NaOH- and NaCl-containing Nafion perfluorosulfonate membranes.⁴ If the lowest frequency peak for the filled membranes is likewise associated with the relaxation of the interfacial polarization of isolated clusters, in this case containing nanometers in extent silicon oxide "networks", the suppression of this peak might then be associated with the eventual intergrowth of these clusters. This might not appear to be an unreasonable mechanistic assignment if the seemingly corresponding low-frequency peak seen in the absorption spectra for the unfilled membranes would not exhibit the same general behavior. Of course, to salvage this notion, one might imagine that both systems would contain clusters of about the same size and having the same protonic charge carriers. As the temperature increases, one might further imagine that the motions of these charge carriers in both systems would eventually become delocalized to such an extent that they are no longer confined within individual cluster boundaries. This view, conveniently of course, is not strongly linked to the chemical composition of either of the clusters. Finally, we are presently unable to offer an explanation for the origin and strange temperature response of the high-frequency peak for either filled or unfilled membranes.

Acknowledgment is made to the donors of the Petroleum Research Fund, administered by the American Chemical Society, for support of this research. We are also

thankful to E. I. duPont de Nemours & Co. for their kind donation of Nafion 117 membranes.

References and Notes

- (1) Nafion is a registered trademark of E. I. duPont de Nemours and Co., Inc.
- (2) Mauritz, K. A.; Storey, R. F.; Jones, C. K. In *Multiphase Polymer Materials: Blends, Ionomers and Interpenetrating Networks*; Utracki, L. A., Weiss, R. A., Eds.; ACS Symposium Series 395; American Chemical Society: Washington, DC, 1989; Chapter 16.
- (3) Mauritz, K. A.; Warren, R. M. *Macromolecules* **1989**, *22*, 1730.
- (4) Mauritz, K. A.; Fu, R.-M. *Macromolecules* **1988**, *21*, 1324.
- (5) Mauritz, K. A.; Yun, H. *Macromolecules* **1988**, *21*, 2738.
- (6) Mauritz, K. A.; Yun, H. *Macromolecules* **1989**, *22*, 220.
- (7) Mauritz, K. A. *Macromolecules* **1989**, *22*, 4483.
- (8) Polder, D.; van Santen, J. H. *Physica* **1946**, *12*, 257.
- (9) Hedvig, P. *Dielectric Spectroscopy of Polymers*; Wiley: New York, 1977; p 293.
- (10) Niklasson, G. A. *J. Appl. Phys.* **1987**, *62*(7), 1987.
- (11) Sher, H.; Montroll, E. W. *Phys. Rev. B* **1975**, *12*(6), 2455.
- (12) Dissado, L. A.; Hill, R. M. *Proc. R. Soc. London* **1983**, *A390*, 131.
- (13) Dissado, L. A.; Hill, R. M. *J. Chem. Soc., Faraday Trans. 2* **1984**, *80*, 291.
- (14) Gierke, T. D.; Munn, G. E.; Wilson, F. C. *J. Polym. Sci., Polym. Phys. Ed.* **1981**, *19*, 1687.
- (15) Starkweather, H. W., Jr. *Macromolecules* **1982**, *15*, 320.
- (16) Huang, Hao-Hsin; Wilkes, G. L.; Mauritz, K. A., unpublished studies.

Registry No. TEOS, 78-10-4; Nafion 117, 66796-30-3.

Application of the "Spectroscopic Ruler" to Studies of the Dimensions of Flexible Macromolecules. 1. Theory

Guojun Liu and J. E. Guillet*

*Department of Chemistry, University of Toronto, Toronto, Canada M5S 1A1.
Received May 17, 1989*

ABSTRACT: This paper explores the feasibility of using the Förster "spectroscopic ruler" relation for measuring the end-to-end distances of flexible organic polymer chains. The experimental techniques for measuring the energy-transfer efficiencies from the naphthalene donors, attached at one end of polymer chains, to anthracene acceptors at the other end of the chains are established. Numerical solutions are obtained for the theoretical expression for energy-transfer efficiencies. Replacing the theoretical energy-transfer efficiencies in the theoretical expression with experimentally measured values should enable one to fit the root-mean-square end-to-end distances of polymer chains.

I. Introduction

The root-mean-square end-to-end distances, R_n , of macromolecules in solution are important measures of the dimensions of polymer coils. Knowledge of R_n is of both experimental and theoretical importance. Three principal methods have been used for the determination of dimensions of macromolecules: light scattering,¹ viscosity,² and diffusion coefficient³ measurements. Determination of inelastic scattered light intensity versus angle yields the radius of gyration, R_G . For long chains, if the correlation between bond pairs diminishes rapidly with sequence separation, R_G is related to R_n by

$$R_G = (1/6)^{1/2} R_n \quad (1)$$

The diffusion coefficient, D , for polymer coils can be mea-

sured by either dynamic light scattering experiments⁴ or measurement of the sedimentation velocity.³ If non-draining coils are assumed, the coefficient D can be related to another effective radius R_D , equal to the hydrodynamic radius, R_H (related to R_G and therefore R_n), through the Stokes relation for a sphere by

$$D = \frac{kT}{6\pi\eta_0 R_D} \quad (2)$$

where kT is thermal energy and η_0 is the viscosity of the solvent. The viscosity measurement makes use of eq 3, first derived by Einstein,⁵ where R_h is the equivalent hydro-

$$\eta_s = \eta_0 [1 + (10/3)N\pi R_h^3] \quad (3)$$

dynamic radius of the nondraining coil, N is the number